



This is a repository copy of *Limitations of processing carbon fibre reinforced plastic/polymer material using automated fibre placement technology*.

White Rose Research Online URL for this paper:  
<http://eprints.whiterose.ac.uk/104178/>

Version: Accepted Version

---

**Article:**

Smith, R., Qureshi, Z., Scaife, R. et al. (1 more author) (2016) Limitations of processing carbon fibre reinforced plastic/polymer material using automated fibre placement technology. *Journal of Reinforced Plastics and Composites*, 35 (21). pp. 1527-1542. ISSN 0731-6844

<https://doi.org/10.1177/0731684416659544>

---

**Reuse**

Items deposited in White Rose Research Online are protected by copyright, with all rights reserved unless indicated otherwise. They may be downloaded and/or printed for private study, or other acts as permitted by national copyright laws. The publisher or other rights holders may allow further reproduction and re-use of the full text version. This is indicated by the licence information on the White Rose Research Online record for the item.

**Takedown**

If you consider content in White Rose Research Online to be in breach of UK law, please notify us by emailing [eprints@whiterose.ac.uk](mailto:eprints@whiterose.ac.uk) including the URL of the record and the reason for the withdrawal request.



[eprints@whiterose.ac.uk](mailto:eprints@whiterose.ac.uk)  
<https://eprints.whiterose.ac.uk/>

# On the limitations of processing CFRP material using automated fibre placement technology

R.P. Smith<sup>1</sup>, Z. Qureshi<sup>1</sup>, R.J. Scaife<sup>1</sup>, H.M. El-Dessouky<sup>1,2</sup>

<sup>1</sup>Composites Centre, AMRC (Advanced Manufacturing Research Centre) with Boeing, University of Sheffield, Sheffield S60 5ZT, UK; <sup>2</sup>Physics Department, Mansoura University, Mansoura 35516, Egypt

## Abstract

Automated fibre placement (AFP) was used to optimise the tow-steering of carbon fibre reinforced polymer (CFRP) whereby the minimum defect-free steering radius ( $R_{\min}$ ) achievable. The results revealed that in the case of the woven ply surface with unheated tool the  $R_{\min}$ , using 1/4 inch tows, is found to be 1,350mm. For the bare tool surface, the tool temperature had to be raised to 30°C in order to achieve the same  $R_{\min}$  of 1,350mm. To attain a seamless transition from part design to manufacture using CAD, AFP was equipped with software tools ([TruPLAN](#) and [TruFIBER](#)). From the results of software validation and steering trials on a variable radius tool having a pre-laid UD ply, it is found that the ability to steer around a tighter radius was a vast asset of the 1/8 inch tow over the 1/4 inch one, which makes it the preferred choice for the more geometrically complex parts.

**Key Words:** Tow; Defects; Process [Modelling](#); Automated fibre placement (AFP)

## For corresponding:

Dr. Hassan El-Dessouky, Email: [h.el-dessouky@sheffield.ac.uk](mailto:h.el-dessouky@sheffield.ac.uk) & Tel: +44(0)1142227674

## Introduction

Traditional manufacturing process for producing carbon fibre reinforced plastic/polymer (CFRP) parts involves hand lay-up of prepreg plies followed by curing in an autoclave. Such methods are labour intensive, time consuming and prone to repeatability and accuracy issues. Increasing demand for producing high volumes of CFRP parts with consistent quality has led to the use of Automated Fibre/Tape Placement (AFP/ATP) systems. With such systems, prepreg plies can be collated automatically and rapidly with a good level of geometric accuracy. The settings of the ATP processing parameters play an important role in determining the mechanical and physical performance of cured parts and determining the optimum process settings is necessary to ensure acceptable part quality.

Fibre steering is not straightforward to interpret, since its limitations depend on other factors such as material tackiness, compacting pressure of AFP roller, layup speed, source of heating and process temperature. Concerning the fibre steering radius, the constraint is mainly caused by fibre in-plane curvature and material width, and may lead to wrinkles and/or buckling out of plane if the turning radius is too small. The presence of buckled tows could negatively affect the laminate quality, therefore a limit on the steering radius is imposed, usually defined in terms of a minimum radius for the centerline of the course<sup>1</sup>. Fibre-course steering radius analysis at the design stage should always be correlated to real sample tests in order to get the empirical knock-down factors, Coriolis software was designed by Blanchard<sup>2</sup> to establish database within the software in order to detect such problem through a geometrical analysis of the in-plane curvature of tow centerline curve, in order to highlight critical areas.

It is known that the defects of tow path positioning by AFP result in course/band to course gap, course overlaps, and tow end placement faults. As an attempt to overcome this problem Researchers at Electroimpact ([www.electroimpact.com](http://www.electroimpact.com))<sup>3,4</sup> presented a combination of accurate articulated robot technology and modular AFP heads provided with a flexible platform (i.e. application roller). This system is used to layup flat charges that have fibre steering and are near net shape. This allows optimisation of fibre direction and reduces waste.

Two composite cylindrical shells, from IM7/8552 carbon-epoxy slit tape, with the same nominal 8-ply  $[\pm 45/\pm \theta]_s$  layup have been produced by Wu KC<sup>5</sup>, where  $\theta$  indicates a tow-steered ply. The AFP machine was used to steer and place the UD prepreg tows onto the circumference of a 17-inch diameter right circular cylinder. One of the shells was made from overlapped tows and the second was produced without overlaps. The shell with tow overlaps shows improved buckling load and stiffness for Y-axis bending when compared to a quasi-isotropic shell. For the case of no overlaps, the gaps between adjacent courses where tows are dropped on the shell without overlaps are more prominent than was predicted during the design stage.

Chen et al<sup>6</sup> carried out both simulation and experimental studies to investigate fibre/tow steering under different processing parameters, such as layup rate and compaction pressure, during the AFP process. Fibre paths were designed using curved fibre axes with different radii as well as a series of sinusoidal fibre paths. The experimental results showed that it was possible to layup fibre paths with minimum steering radii of 114 mm. In addition to this the fibres of the tow can be steered in a relatively tight radius without buckling or wrinkling by allowing differential feed rates and cut/restart tows. This is because the feed rate of each tow within the course/band can be individually controlled, allowing a curved course with tows at the outside of the curve to be fed faster than those on the inside of the curve<sup>7,8</sup>.

Manufacturing FRP with constraints such as a minimum fibre steering radius, several designs were generated by Klomp-de Boer<sup>9</sup> and compared to the baseline constant stiffness layup, which was a quasi-isotropic lay-up. Dassault manufactured and tested both the baseline and optimal parallel-path variable stiffness panel (same materials and equal thickness) successfully with the steered configuration achieving over 50% higher ultimate load. Comparing the failure strains at the holes' edge of both panels it was found that these are comparable. The fabricated steered panel was found to have a 5% higher fibre volume fraction. The agreement between predicted load carrying capability and test results was excellent. Based on the predictions for the shifted-path steered design, it was reported that up to 35% further increase of load carrying capability can be achieved.

As an attempt to avoid the fibre buckling and allow tows to steer within the course using AFP, Rhead et al<sup>10</sup> reported that by allowing gaps to form between consecutive courses, the fibres could freely steer with less constraint resulting in improved buckling. In ref. 10 two composite samples (Hexcel M21/IMA-12k prepreg CFRP tows) containing tow gaps were subject to compression after impact testing. Tow gaps in sample A were located close to the impact face. Tow gaps in sample B were located directly under the impact site near the nonimpact surface and caused significantly more surface deformation than in sample A. They found that the impact damage was less severe for sample B and the damage tolerance was 14% better for B as both the initial delamination during impact and delamination growth during compressive loading were inhibited.

Generally, various methods such as staggering parallel path, shifted path, tow-overlap and tow-drop and the choice of the coverage parameter, haven been developed to minimise the influence of defects and improve the mechanical properties of the tow-steered laminates. Parallel paths require a change in fibre path curvature which may subsequently trigger the constraint on minimum steering radius, Gaps and overlaps occur when paths are shifted from the original path along a fixed axis. Overlaps can be avoided by dropping tows along the fibre path. Unfortunately these methods cause the laminate to become locally asymmetric and unbalanced leading to low strength and poor surface quality. The influence of such defects in terms of the mechanical performance of tow-steered structure is not yet well understood<sup>11-13</sup>.

Fayazbakhsh et al<sup>14</sup> used AFP to manufacture a variable stiffness laminates, during the manufacturing process, defects appearing in the form of gaps and/or overlaps emerge within the composite laminate. MATLAB subroutines were developed to capture the location and level of the defects whereby a new method, called defect layer, was proposed to characterise the change in properties of each layer in the composite laminates that results from the occurrence of gaps and overlaps. The results show that by incorporating gaps in the laminates the buckling load improvement resulting from tow steering reduces by 15% compared to the laminates where gaps are ignored. A maximum improvement of 71% in the buckling load over the quasi-isotropic laminates can be observed for a variable stiffness laminate built with a complete overlap strategy. In another study<sup>15</sup> it is reported that the optimum mechanical properties of composite laminate with curvilinear fibre is

determined using finite element analysis as a solver within their optimization framework. A metamodel was proposed to reduce the time for analysis and thus for optimization. A set of metamodeling techniques for the design optimization of composite laminates with variable stiffness were examined. Three case studies were considered. They claimed that the most accurate and robust models in exploring the design space are Kriging and Radial Basis Functions. The suitability of Kriging is the highest for a low number of design variables, whereas the best choice for a high number of variables is Radial Basis Functions.

In this work, a parametric study on the steering processability and limitations of individual tow-bands or courses was carried out using the ADC-AFP software. The Magestic software tools ([TruPLAN](#) and [TruFIBER](#)) were used to study the steering of tows in a sub/full ply. For validating the software used, cross-angle plies were laid onto a varying radius tool, following by manufacturing of a complex 3D spar component for demonstration.

## 1. Materials

For the steering trials, ¼ inch wide unidirectional CF prepreg [tows](#) MTM44-1/HTS5631 (145g/m<sup>2</sup>) [were](#) used. HTS-5631 is high strength aerospace grade 12k carbon fibres. MTM44-1 is a high performance, 180°C (356°F) curing, and toughened epoxy resin formulated for the production of primary and secondary aircraft structures. For the woven ply surface, woven sheet of MTM57/CF0100 (280g/m<sup>2</sup>-4x4 twill-3k-T300) prepreg was used. MTM57 is based on a 120°C curing epoxy matrix resin designed for component manufacture.

In addition ¼ inch tows from different materials MTM44-1/IM7 and 977-3/IM7 were used and a narrower tow of 1/8 inch wide from the same material above (MTM44-1/HTS5631) was also used for comparing the steering trials and part manufacture. All materials were developed by the advanced composites group (ACG) and Cytec.

## Equipment

### *Automated fibre placement (AFP) system*

AFP systems are currently an area of interest for the aerospace industry due to their ability to improve part quality, repeatability and production rate. In addition, automating the composite lay-up process reduces labour cost and cycle time. In order to obtain good part quality using the AFP system, the effects of process parameters (factors) on the part's physical and mechanical properties need to be considered. Process parameters that can affect the part performance include roller compaction force ( $F_R$ ), material deposition/roller speed ( $V_R$ ), nitrogen gas temperature ( $T_{NG}$ ) and tool/substrate temperature ( $T_T$ ) (see Fig. 1). Additional details on the AFP technology used in this work can be found in references 16-18<sup>16-18</sup>.

### *Software tools: TruPLAN and TruFIBER*

The software provided by Magestic Systems Inc.<sup>19</sup>, consists of two modules, TruPLAN and TruFIBER that are embedded into the composite part design (CPD) workbench within CATIA V5 and DELMIA software, respectively. TruPLAN is the initial design module of the software, which allows the user to determine the effects of changing process variables, such as material, tow size and layup strategy on the deposition process. Material analysis such as wrinkling, steering and compaction can be performed. Once a suitable layup strategy is identified, it is passed to TruFIBER (DELMIA), which is the machine programming module of the software.

In TruFIBER, the fibre paths are analysed further and collision avoidance checks are performed to ensure safe operation. In terms of inputs, part operations and machine settings (robot type, reference point, safety planes, etc.) are defined. Fibre placement parameters (number of tows, tow width, feed rates) and operations (lay-up direction, roller information, on/off part motion, collision model, etc.) are defined next. Final stages in TruFIBER involves tool path computation, detailed review and editing to ensure that the lay-ups are correct, roller conformation is reasonable and robot motion is as expected.

## Experimental

### *AFP parametric trials on the steering of discrete tow-bands*

A number of steering experiments were performed to determine the minimum tow-steering radius ( $R_{\min}$ ) for which minimal or no material defects are obtained. Tow fold-over was the main defect/response monitored throughout the experimental trials. Figure 2 shows a schematic diagram of the steered set of tows (8 of ¼ inch wide tape).  $R_{\min}$  (values are given in following section: results and discussion) was measured from the central line that separates the 8 tows into 2 bands of 4-tow each.

Based on the initial pilot steering experiments, default parametric values were established for defining the constants for the steering trials. A defect-free radius was defined as the minimum steered radius that contained no tow fold-overs, but slight compressible wrinkles were acceptable. The obtained (default) setting given in Table 1 was to determine the  $R_{\min}$  by steering the tows onto a bare tool and woven ply surfaces. A woven prepreg ply was selected in order to represent a typical ply surface onto which tows would be steered.

In order to maximize and optimize the influence of AFP factor settings on the tow-steering process, the effects of tool temperature ( $T_T = 20, 25, 30, 35^\circ\text{C}$ ), nitrogen gas temperature ( $T_{\text{NG}} = 50, 100, 150^\circ\text{C}$ ) and roller speed ( $V_R = 100, 200, 300\text{mm/s}$ ) were studied. In the case of studying the effect of tool temperature the same default factor settings (Table 1) were used except for the  $T_{\text{NG}}$  value, which was reduced to  $50^\circ\text{C}$ . The reason for this was to decrease the heat experienced by the AFP head and thereby reduce the risk of any material getting stuck inside the tow guides. The heated tool provided sufficient energy to increase the material's tackiness, allowing it to stick to the tool.

The 4-tow AFP head was used for the tow-steering studies. The head can process four of ¼ inch (6.35mm wide) tows with the material bobbins installed onto the head, allowing the material travel distance to be minimal. A flat tool, measuring of 1300x800x10mm, was used for the steering trials. For heating the tool, a silicone heater mat, measuring of 1160x700mm with 3kW power rating, was bonded to the bottom surface of the tool.

### ***In-plane steering trials***

The TruPLAN and TruFIBER upgraded- AFP system was used to perform all steering trials and part manufacture. Both 12-tow 1/8 inch and 4-tow 1/4 inch deposition heads were used. In this case different setting of the processing parameters was used throughout the trials, unless otherwise stated as listed in Table 2.

In order to feed the TruPLAN for performing the steering analysis on the fibre path,  $R_{\min}$  was determined for a range of commonly used materials and tow widths by laying multiple arcs of material, continually decreasing the radius, until the failure criteria was observed as explained in Table 3. Two  $R_{\min}$  values were used by TruPLAN, these are called the 'warning' and 'limit' steering radius. The 'warning' value is used to show areas of concern which should be investigated further, whereas the 'limit' value will flag predicted defects, and should therefore not be exceeded. The failure criteria for these two values are given in Table 3.

### ***Software/analysis validation using variable radius tool***

The fibre steering analysis tools was experimentally validated, using the data generated from in-plane steering trials to set the limits within the software. For these experiments, a variable radius tool (Fig. 3) was used, allowing a range of steering radii to be projected over complex geometry. Plies were programmed at all four principle orientations ( $0^\circ$ ,  $+45^\circ$ ,  $-45^\circ$ ,  $90^\circ$ ) and analysis was performed on the resulting fibre path. Areas predicted to contain defects were noted and physical experiments were then performed to see if the predictions were accurate.

Figure 4 exhibits the results of the steering analysis carried out for a  $0^\circ$ ,  $90^\circ$  and  $+45^\circ$  fibre orientation. In all instances there were no signs of steering defects on the part. Positioning of the rosette (reference coordinate system) is critical to ensure an accurate output for the simulation.

### ***Manufacturing of spar demonstrating component***

For this part, the entire design and manufacture process was carried out using the information gathered from the software validation and analysis of tow steering trials. A rear spar with various levels of geometric complexity was selected as a final demonstration part. [Figure 5](#) shows the CAD model of the spar component, which exhibits the various boundaries created to keep the fibre angle deviation to a minimum and reduce steering over the complex surfaces and radii. It was also to further validate the results conducted from the steering trials and to assess the validation of the collision software using such complex 3D geometry. In addition, the fibre placement editor within the [TruFIBER](#) software was used to manipulate plies, bands and tows and the manual dictate head angles and vectors were used to optimise for roller compaction and collision avoidance.

Due to the complexity of the spar created by tight radii, double curvatures and surface joggles, there are a number of strategies in which the fibre propagation can be achieved within the TruPLAN software. In this instance, “constant angle offset” was chosen which propagated to the input limit for angle deviation, but did not overlap the tows or create gaps between the tows. The Constant Angle propagation mode consists of creating courses whose centre line follows the direction of material specified for the ply. In other words, the tangent to the centre line at any point is equivalent to the reference vector for the ply projected onto the tangent plane of the support and rotated around the normal to the specified orientation. The Constant Angle Offset propagation mode is similar to the Constant Angle propagation mode in the sense that the first course of a ply generated with this method has a constant angle centre line. This first course is generated through the start point given for the ply. All other courses are adjacent to the previous course and are parallel offsets of the centre line of the first course. For this reason, the large full surface plies were divided into multiple sub-ply. This enabled the fibre orientation not to deviate more than the specified 3 degrees from nominal. Creating smaller sub-ply also limited the amount of steering created in the tows ([Fig. 6a](#)). This is because for every sub-ply, a separate seed point (starting point/location for placing the tow and to begin the calculation) can be allocated from which the fibre propagation starts. By strategically positioning the seed point, the steering was limited within that specific sub-ply. Originally the multiple sub-ply boundaries were created to combat the fibre angle exceeding the max allowable deviation.

By simply using the full plies outer periphery as one complete boundary, only one seed point was available across the whole part, thus creating minimal deviation and steering in very close proximity to the seed point. However, as the fibres propagated further away across the part surface, the deviation became further from nominal and the steering of the fibre increased dramatically (Fig. 6b).

## Results and discussion

Figure 7a shows eight steered tows on the bare tool with a few fold-overs. Two bands (8 tows) were steered for each radius to check the repeatability of the process. The second band was used to record the data as it was observed that the first band's tackiness was reduced due to the material resting inside the cooled head for too long. Instead of the bare tool an initial MTM57/CF0100 woven ply was used to steer the tows onto as shown in Figure 7b. A number of steering radii, ranging from 1,000mm to 2,250mm, were tried until a defect-free radius was obtained for all the steering settings as detailed above. Using the setting given in Table 1 and the tow-steering trials carried out, it is found that the defect-free radii ( $R_{min}$ ) for the steered tows on bare tool and woven ply surfaces are found to be 2,000mm and 1,350mm, respectively.

Figure 8 shows typical defected and defect-free bands of steered tows on aluminium plate, the top one exhibited multiple of fold-overs in which the fold-over lengths of inner tows were generally longer and wider than that of the outer tows. The middle band has only a fold-over of the inner steered tow leading to a gap between the tows. A band with defect-free steered tow with  $R_{min} = 2,000\text{mm}$  is shown at the bottom of the figure.

In the case of tow-steering on a woven ply (Fig. 9), it is found that a multiple of defect-free (no fold-over) steered tow-bands were achieved. A few minor wrinkles were observed on some steered tows and were not classified as a failing criteria as such wrinkles were compressible and would normally be flattened-out by the subsequent ply. A range of steering radii was successfully manipulated and measured as shown in Figure 9. The trail of steering tow of radius 1,250mm was not successful as a defect (fold-over) was observed (see the zoomed in image in Fig. 9). The minimum tow-steering achieved was 1,350mm on the woven ply.

The lower defect-free steering radius ( $R_{min}$ ) was obtained for the woven ply than the bare aluminium surface. This is mainly because the woven ply provides additional tack to the steering tows, enabling them to stick better with fewer defects. Due to no tack provided by the bare aluminium tool surface, the tows start to fold-over more even at higher steering radii.

In the case of changing the temperature of nitrogen gas ( $T_{NG}$ ), it is observed that the minimum defect-free steering radii ( $R_{min}$ ) achievable onto a woven ply are 2,250mm, 1,750mm and 1,350mm at 50°C, 100°C and 150°C, respectively. [Figure 10](#) shows the defected steered tows of 1,350mm radius using  $T_{NG}$  of 50°C and 100°C. It is concluded that as the  $T_{NG}$  is increased from 50°C to 150°C, the minimum defect-free ( $R_{min}$ ) of tow-steering onto a woven ply surface decreases from 2,250mm to 1,350mm as shown in [Figure 11](#). Increasing  $T_{NG}$  reduces the resin viscosity as more heat energy is provided. This reduction in viscosity increases the tackiness of the incoming tows and the substrate ply, enabling the steering tows to stick better. As the tows adhere better to the substrate ply, the number and severity of fold-overs is reduced.

The effect of roller speed ( $V_R$ ) on the  $R_{min}$  by steering the tows onto a woven ply surface was studied at 100, 200 and 300mm/s. It is noticed that for speeds of 100mm/s and 200mm/s,  $R_{min}$  of 1,750mm was obtained, but when the speed was increased to 300mm/s, the  $R_{min}$  increased to 2,000mm as shown in [Figure 12](#). This is due to the increasing shear rate of the tows and less compaction time available at higher speeds. The combination of high shear rate and low compaction time leads to more fold-over defects at lower steering radii. Therefore, a higher  $R_{min}$  is obtained for higher  $V_R$ . For speed settings of 100mm/s and 200mm/s, the  $R_{min}$  remained the same. This was due to minimal difference in the speeds achieved for both speed settings.

In order to investigate the effect of tool temperature ( $T_T$ ) on  $R_{min}$  using bare aluminium tool surface, the tool temperature was varied from 20°C (room temperature) to 35°C with an increment of 5°C. As the  $T_T$  was increased from 20°C to 30°C,  $R_{min}$  was exponentially decreased from 2,250mm to 1,350mm. There was no improvement in  $R_{min}$  as the  $T_T$  was increased from 30°C to 35°C as shown in [Figure 13](#). In the case of using the woven ply surface, no improvement in  $R_{min}$  was found when the  $T_T$  was increased from 20°C to 35°C.

The  $R_{min}$  value remained constant at 1,350mm for all  $T_T$  settings. This implies that a tool temperature  $T_T$  of only 20°C is sufficient to obtain  $R_{min}$  of 1,350mm for tows being steered onto a woven ply. However, the  $R_{min}$  was reduced from 2,250mm to 1,350mm using the same  $T_T$  range for the bare aluminium surface. As stated before, increase in heat energy transferred into the resin system, via increased tool or gas temperature, reduces resin viscosity and provides more tack. This helps the tows to adhere better to the surface and thereby reduces the defects.

Table 4 summarises the key findings for the tow steering trials conducted from the parametric study. The minimum defect-free radii ( $R_{min}$ ) for bare tool and woven ply surfaces were 2,000mm and 1,350mm respectively without heating the tool. For bare tool surface, the  $R_{min}$  was reduced to 1,350mm as the tool was heated to 30°C. For woven ply surface,  $R_{min}$  was unaffected by the tool temperature for the range investigated.

Table 5 shows the steering trial results for different material types and widths. As expected the 1/8 inch wide tows exhibited lower  $R_{min}$  values (500mm) than the 1/4 inch wide tows. This is mainly due to the ability of narrower tows to withstand higher shearing before folding over starts when compared to the wider tows. MTM44-1 resin system exhibited lower  $R_{min}$  values (1000mm) when compared to the 977-3 resin system of the same tow width. The reason for this was the higher tackiness (resin rich surface) of the MTM44-1 resin system than the 977-3, allowing the MTM44-1 material to stick better to the substrate before allowing for tow to fold over. [Figures 14 and 15](#) show a sample of steered tows and tow fold over respectively.

[Figure 16](#) shows the ply steering results, for variable radius tool, obtained during experimental trials and how they compare to the TruPLAN results. It is found that the analysis created in TruPLAN, using the steering parameters set, appear [similar](#) to the actual fibre placed part as shown at the tow-courses 16 and 17. The white line represents the centre line for course 16. [Figure 17](#) shows the steering results for a -45° ply for tow-bands 23-24. No steering issues (i.e. fold overs or wrinkles) were observed during the layup process, which also validated the TruPLAN results for those specific bands. Although the tow steering shown in [Figures 16 and 17](#) were applied at the same angle, the fibre paths behave differently. This is due to the fact that the examples in [Figure 16](#) were at an excessive

distance from the seed point for the ply thus creating steering in the part which was used to prove out the simulation versus actual part. [Figure 17](#) is an example of a section near the seed point where the fibre angle and steering are still within expectable limits. [Figure 18](#) shows steering results for +45° ply, bands 10-12 with considerable steering defects obtained from both experimental trials and TruPLAN simulations. This implies that the software predictions matched the experimental observations accurately.

In general, [Figure 16](#) shows that the simulation is correct for the steering analysis and the actual part manufacture is true to the analysis and exhibits steering as well. [Figure 17](#) is an example of an area exhibiting no steering issues in simulation and is a match with the part manufacture. [Figure 18](#) shows how the simulation has not accounted for the overlapping of the tows at the end of the bands due to the lack of tow control once the tows have been cut.

[Figure 19](#) shows the spar part with ±45°, 0° and 90° plies set out in multiple sections to realign the fibre paths at certain intervals. Although the Spar component had been previously manufactured using the standard AFP in another work, its manufacture using the new fibre placement software represented a steep difference from the previous trials. The main issues, challenges and successes encountered during the programming and manufacture of the part are listed below:

- Steering defects could not be completely removed in programming so manual intervention was required during manufacture to rectify poor tow deposition. This issue stems from the fact that tows were being forced to steer away from the geodesic path quite severely.
- ¼ inch tows were used for the manufacture of the Spar component which created steering issues which were not evident when using 1/8 inch tows which were used on the previous manufacture of the Spar component
- Erratic movement of the machine head during manufacture on some of the complex areas of the mandrel would result in a head collision fault stopping the AFP machine. This was a result of the head moving past the internal cut off sensor. No collisions occurred but the machine would stop and plies needed reprogramming to overcome the issue.

## Conclusion

The fundamental differences between the 1/8 inch and 1/4 inch tows became very evident during the steering trials, with the 1/8 inch tow achieving a steering radius far lower than the 1/4 inch tow ( $R_{\min}=1,250\text{mm}$ ). The values of  $R_{\min}$  for 1/8 inch and 1/4 inch tows were 500mm and 1,250mm respectively. This will put the 1/8 inch in a far better position to manufacture parts with a greater complexity. Historically, the only disadvantage to using 1/8 inch fibre to using 1/4 inch fibre tow is the material handling from the AFP machine. The 1/8 inch tow is notoriously difficult for the machine to process through its guides and rollers without creating twists, buckles or jams in the end effector, which all result in process down time for rectifying the issue. This issue seems to be handled significantly better with the 1/4 inch tow deposition. This is due to the material handling being easier due to its surface area, as well as the improvements made to the current iteration of Fibre Placement Head. The manufacturing of a complex 3D part was demonstrated ([Figure 20](#)) to ensure the integration of Magestic and the Automated Dynamics packages.

## Acknowledgment

The authors would like to thank the AMRC's partners for their continuous support and feedback during the course of this project. Special thanks go to the GE Aviation System Ltd ([www.geaviation.com](http://www.geaviation.com)) for using their demonstrating tool and help.

## References

1. Blom AW, Kang LS, Vandenbrande JH. Fiber Placemenet Optimization For Steered- Fiber Plies. Patent No. US 2014/0288893 A1, Boeing, Chicago, US.
2. Blanchard Y. Composites design optimization for automated fibre placement. In: SAE Aerospace Manufacturing and Automated Fastening Conference & Exhibition. Utah, Sep, 2014.

3. Jeffries K. Enhanced Robotic Automated Fiber Placement with Accurate Robot Technology and Modular Fiber Placement Head. SAE Int. J. Aerosp 2013;6(2). doi:10.4271/2013-01-2290.
4. Wells D and Walker A. Integrating ultrasonic cutting with high-accuracy robotic automatic fiber placement for production flexibility. In: SAMPE Tech 2014, Seattle.
5. Wu kC, Tatting BF, Smith BH, Thornburgh RP. Design and Manufacturing of Tow-Steered Composite Shells using Fiber Placement. In: 50th AIAA/ASME/ASCE/AHS/ASC Structures, Structural Dynamics, and Materials Conference. California, May, 2009. DOI: 10.2514/6.2009-2700
6. Chen J, Chen-Keat T, Hojjati M, Vallee AJ, Oceau MA, Yousefpour A. Impact of layup rate on the quality of fiber steering/cut-restart in automated fiber placement processes. Science and Engineering of Composite Materials 2015; 22:165-173.
7. Schueler K, Miller J , Hale R. Approximate Geometric Methods in Application to the Modeling of Fiber Placed Composite Structures. Journal of Computing and Information Science in Engineering 2004; 4: 251-256.
8. Vickers JH, Pelham LI. Automated fiber placement composite manufacturing: The mission at MSFC's Productivity Enhancement Complex. In: Technology 2002 The Third National Technology Transfer Conference and Exposition. Alabama, 2002;2: 255-261.
9. Klomp-de Boer R. Automated Preform Fabrication by Dry Tow Placement. In: National Aerospace Laboratory NLR, NLR-TP-2008-789, SAMPE Tech. Texas, October, 2011. P.17-20.
10. Rhead A T, Dodwell T J and Butler R. The effect of tow gaps on compression after impact strength of robotically laminated structures. Computers, Materials and Continua 2013; 35: 1-16.
11. Salcines OF, [PhD thesis](#) on. Analysis of process-induced defects on steered-fiber panels for aeronautical applications. University of Girona 2014, Spain.
12. IJsselmuiden ST, [PhD thesis](#) on. Optimal design of variable stiffness composite structures using lamination parameters. Delft University of Technology 2011, Netherlands.

13. Khani A, IJsselmuiden ST, Abdalla MM, Gürdal Z. Design of variable stiffness panels for maximum strength using lamination parameters. *Composites: Part B* 2011;42: 546-552.
14. Fayazbakhsh K, Nik MA, Pasini D, Lessard L. Defect layer method to capture effect of gaps and overlaps in variable stiffness laminates made by Automated Fiber Placement. *Composite Structures* 2013;97: 245-251.
15. Nik MA, Fayazbakhsh K, Pasini D, Lessard L. A comparative study of metamodeling methods for the design optimization of variable stiffness composites. *Composite Structures* 2014;107: 494-501.
16. Sonmez FO, Akbulut M. Process optimisation of tape placement for thermoplastic composites. *Composites Part A: Applied Science and Manufacturing* 2007;38: 2013-2023.
17. Mee K, Kilham T, Scaife R, Hodzic A. Application of AFP to Structural Aerospace Components utilising Out of Autoclave Materials. In: 32nd SAMPE Europe International Technical Conference & Forum. Paris, March, 2011. p.28-29.
18. Qureshi Z, Swait T, Scaife R, El-Dessouky HM. In-situ consolidation of thermoplastic prepreg tape using automated tape placement technology: potential and possibilities. *Composites: Part B* 2014;66:255-267.
19. Moruzzi M, Maclean D. Comprehensive cost analysis of the tradeoffs between design intent and applicable manufacturing strategies. Technical paper, Magestic Systems Inc. 2015, <http://s405481842.initial-website.com>.

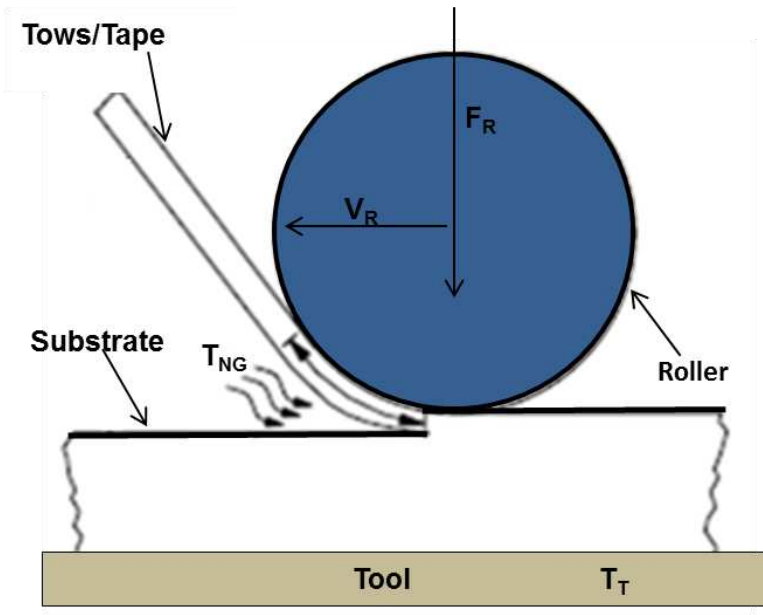


Figure 1. AFP processing parameters

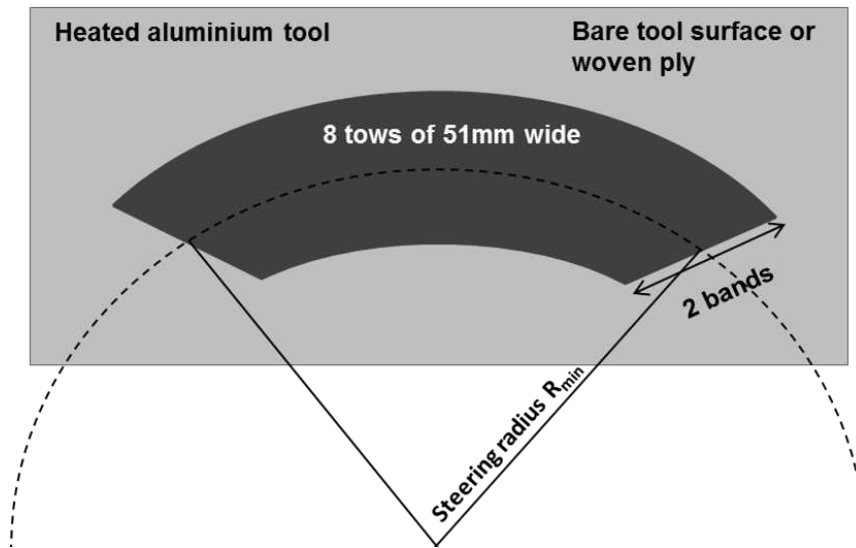


Figure 2. Schematic of steered tows within a band/course

**Table 1.** AFP setting used

Parameter	Default Values
Roller speed, $V_R$ (mm/s)	200
Roller Compaction Force, $F_R$ (lbs)	50
Tow tension (N)	3.5
Nitrogen Gas Temperature, $T_{NG}$ ( $^{\circ}C$ )	150
Nitrogen Gas Flow Rate, $\dot{V}_{NG}$ (lpm)	60
Tool Temperature, $T_T$ ( $^{\circ}C$ )	20 (Room temp)

**Table 2.** AFP Processing Parameters

Variable	Setting
AFP Head(s)	¼" and 1/8" where indicated
Tool	Release Aluminium flat plate tool
Speed, $V_R$ (mm/s)	300
Roller Compaction Force, $F_R$ (lbs)	80
Nitrogen Gas Temperature, $T_{N_2}$ ( $^{\circ}C$ )	150
Nitrogen Gas Flow Rate, $\dot{V}_{N_2}$ (lpm)	100
Tool Temperature, $T_T$ ( $^{\circ}C$ )	Room temperature (20 $^{\circ}C$ )

**Table 3.** Tow steering failure criteria

Defect Type	Warning	Limit
Fold	Any fold	Any fold
Gap / Overlap width	0.5 – 1mm	>1mm
Wrinkle height	<1mm	>1mm



**Figure 3.** Variable radius tool

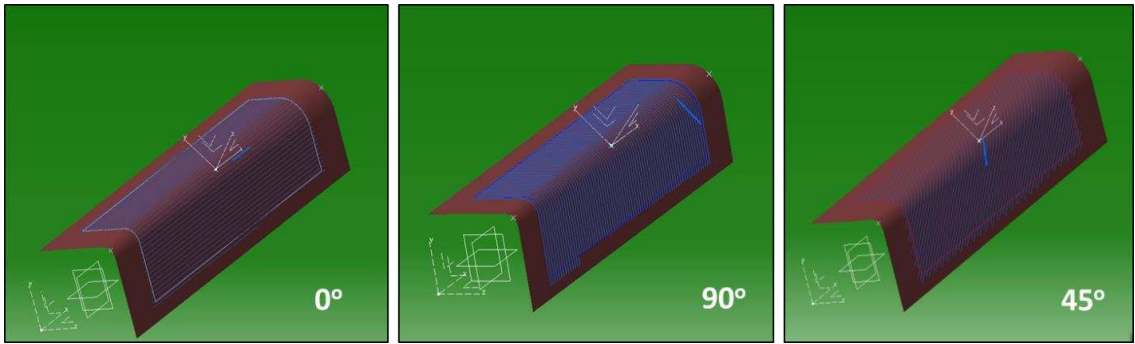


**Figure 4.** 0°, 90° and +45° plies steering analysis

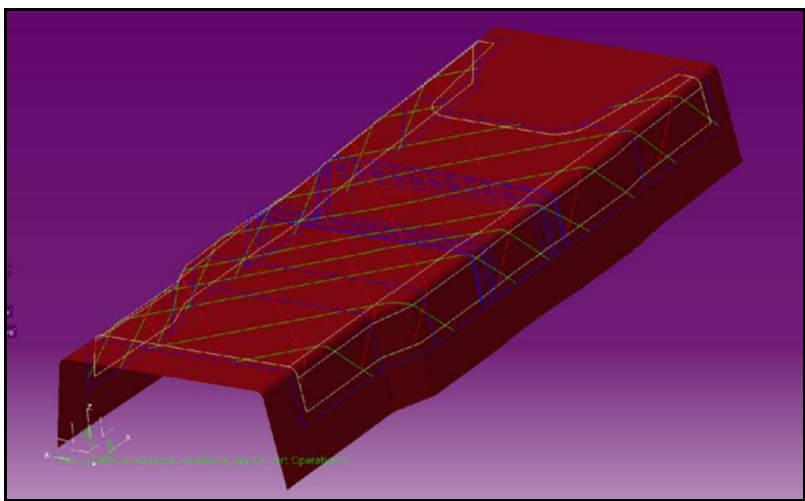


**Figure 5.** Spar CAD model with boundaries defined

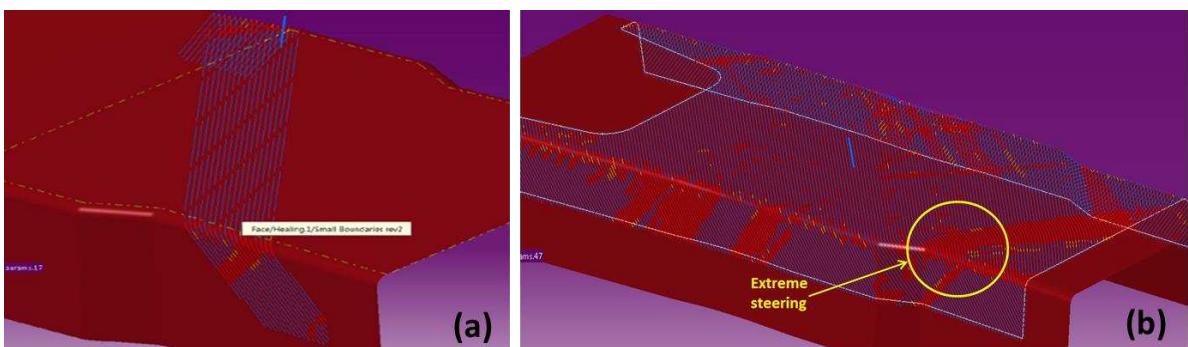


**Figure 6.** a) Sub-ply steering analysis and b) Steering analysis for full ply with only one seed point

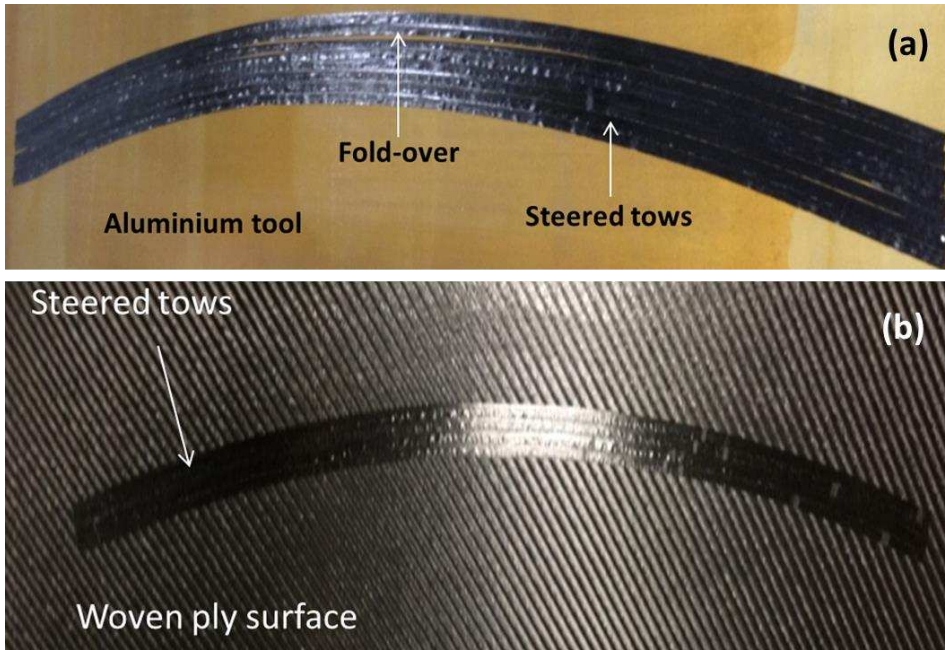


**Figure 7.** a) Steered tows (2 bands) on bare aluminium tool surface and b) Steered tows (one band) on woven ply

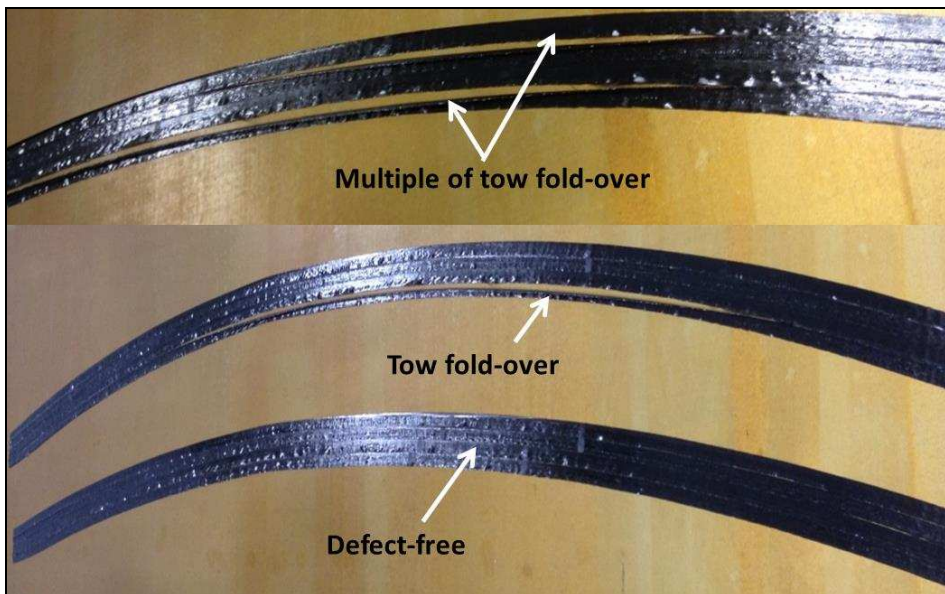


**Figure 8.** Steered tows on aluminium plate

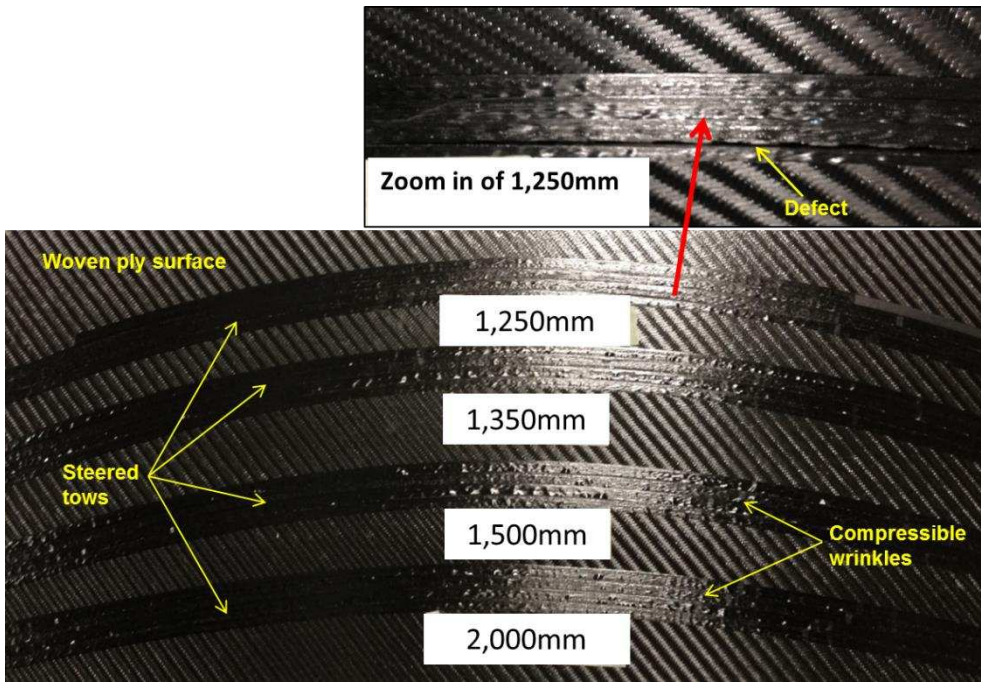


**Figure 9.** Steered tows on woven ply at  $T_{NG} = 150^{\circ}\text{C}$  (Table 2). Radii from 2000mm to 1350mm are acceptable but 1250mm is not.

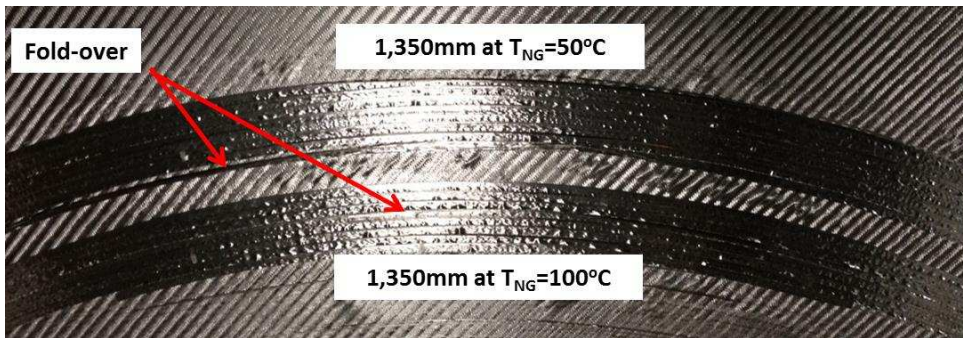


**Figure 10.** Steered tows on woven ply at different  $T_{NG}$

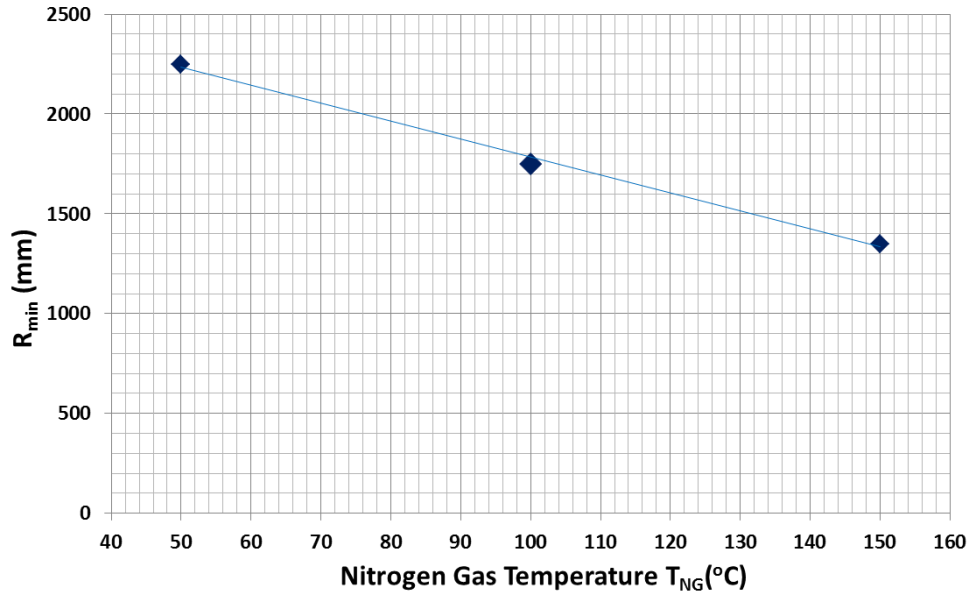


**Figure 11.** Effect of  $T_{NG}$  on defect-free min steering radius ( $R_{min}$ ) onto woven ply

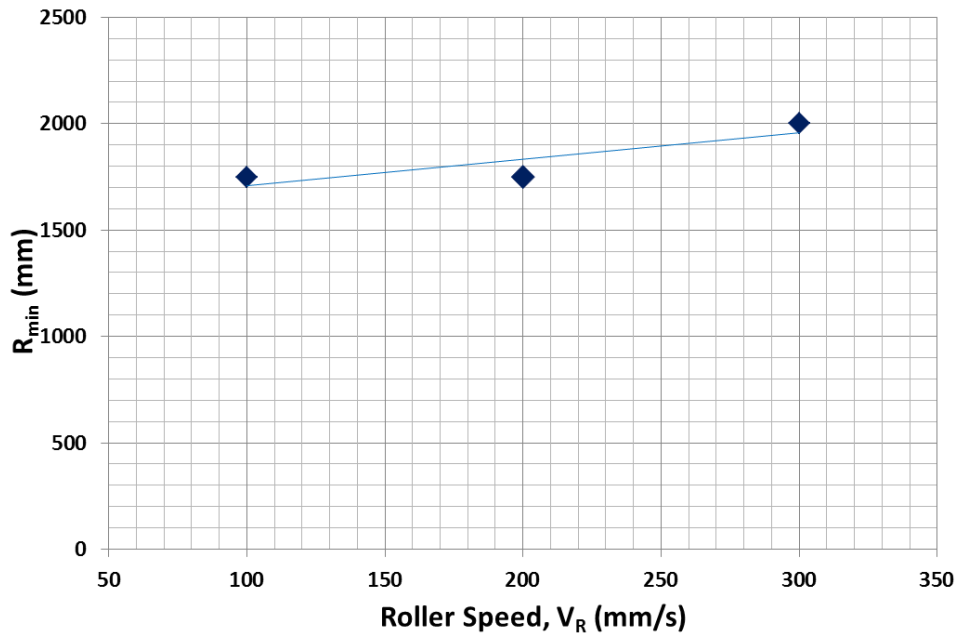


**Figure 12.** Effect of roller speed on defect-free min steering radius ( $R_{min}$ ) onto woven ply

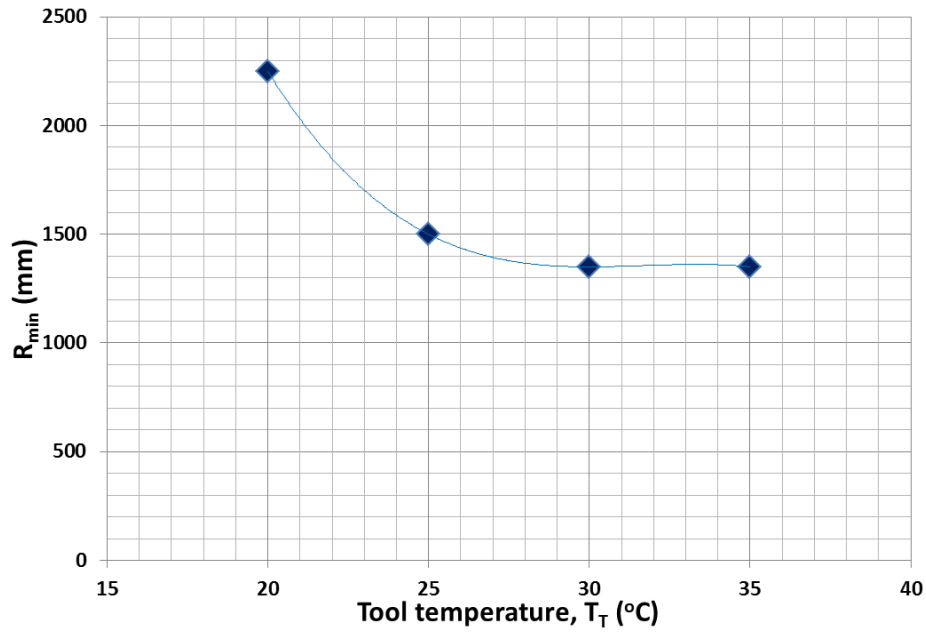


**Figure 13.** Effect of tool temperature  $T_T$  on defect-free min steering radius ( $R_{min}$ ) using bare tool surface

**Table 4.** Summary of the results of the discrete-tows steering parametric trails

Tool type and conditions		$T_{NG}$ (°C)	Min steering radius without defects, $R_{min}$ (mm)
Non-heated tool	Bare tool	150	2,000
	Woven ply	150	1,350
Heated Tool	Bare Tool	50	1,350 at $T_T = 30^\circ\text{C}$
	Woven Ply	50	1,350

**Table 5.** Summary of the results of ply steering trials on a bare surface with pre-laid UD ply

Material	Radius at 1 <sup>st</sup> defect (mm)	Comments
MTM44-1/IM7 1/4"	1,000	1,000 mm limit (gaps) 1,250 mm warning folding at ends
MTM44-1/HTS 1/4"	1,250	1,250 limit (fold), 1,375 warning no distortion (note overlap at the end)
977-3/IM7 1/4"	1,250	1,250 limit (fold), 1,375 warning no distortion
MTM44-1/HTS 1/8"	500	Achieved 300mm

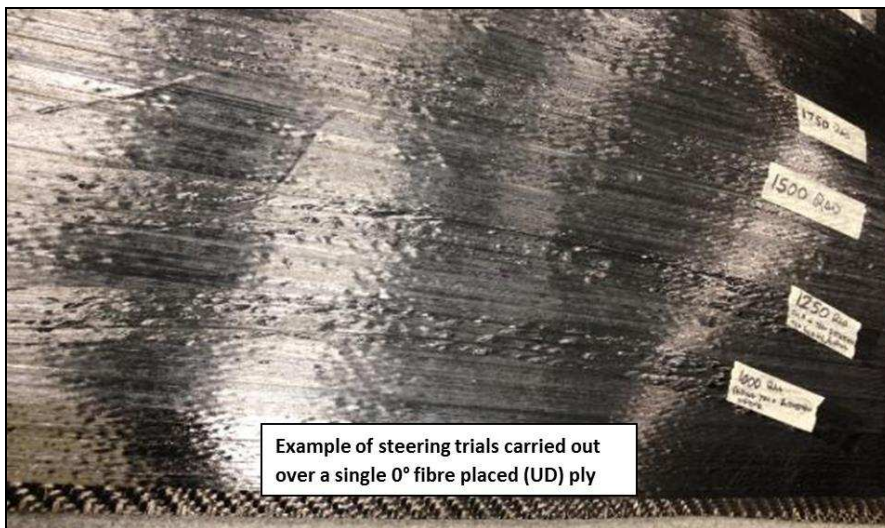


**Figure 14.** Steered tows for 977-3/IM7 (1/4 inch)



**Figure 15.** Typical tow fold-overs

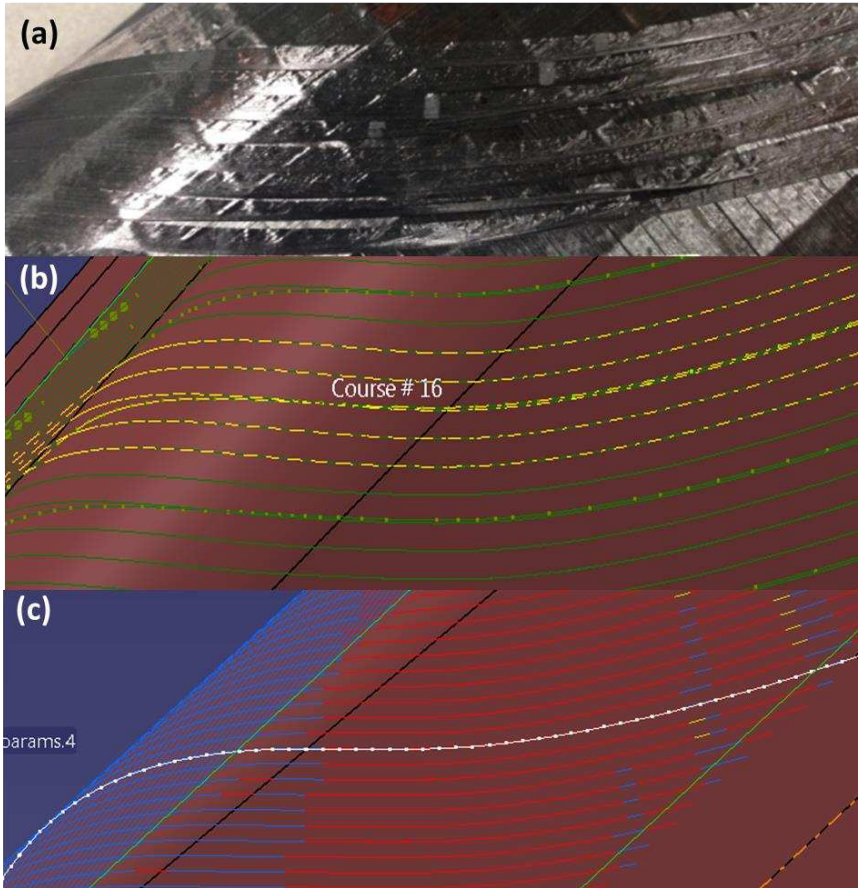


**Figure 16.** TruPLAN Steering Results, a) Fibre placed part with relevant courses/bands (16-17) in the case of  $-45^\circ$  ply b) Simulation from TruFIBER for layout (courses 16-17), c) Simulation from TruPLAN for steering (white line represents centre line for course 16)

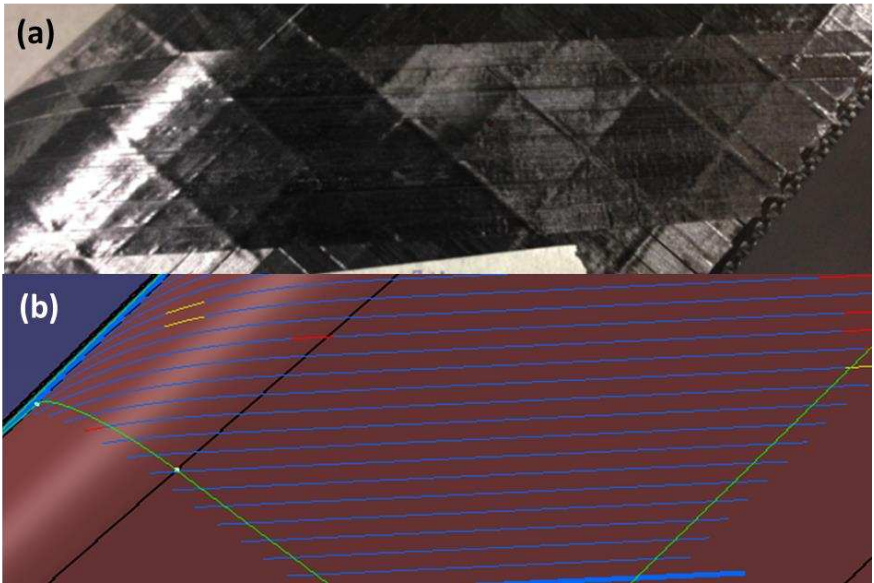


**Figure 17.** TruPLAN Steering Results for Courses 23-24, a) Fibre placed part with no steering issues for bands 23-24 in the case of  $-45^\circ$  ply b) Simulated part with steering analysis showing no steering defects

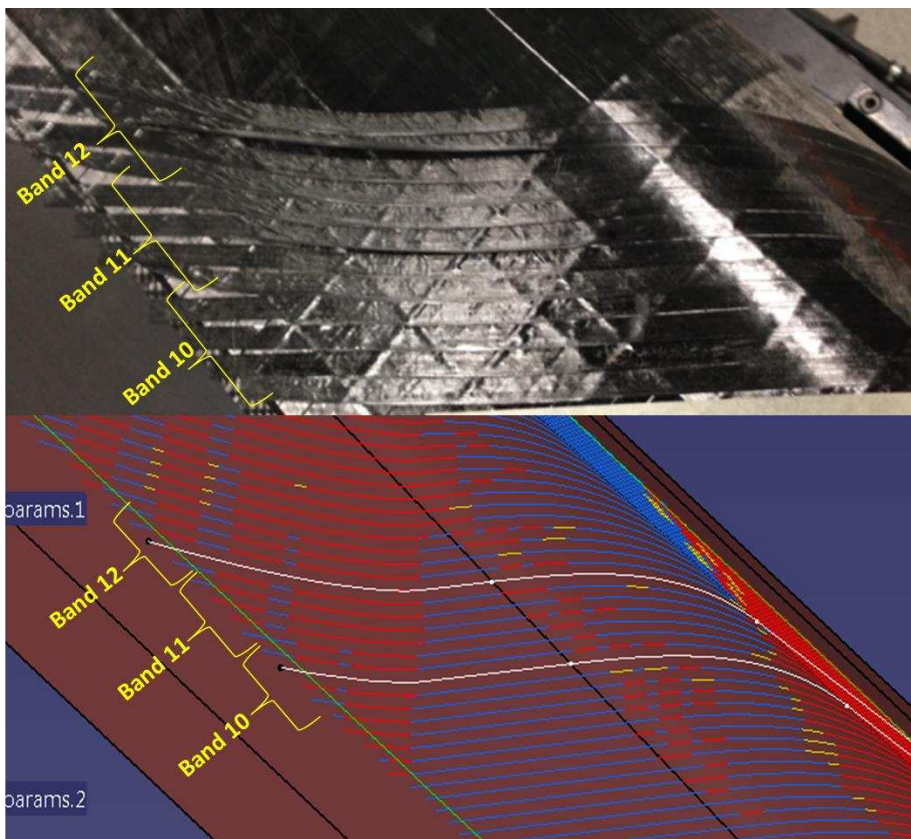


**Figure 18.** Steering results for  $+45^\circ$  Ply, Bands 10-12, a) Fibre placed part exhibiting considerable steering defects (Courses 10-12), b) Simulated part in TruPLAN steering analysis exhibiting considerable steering defects in the same region (courses 10-12)

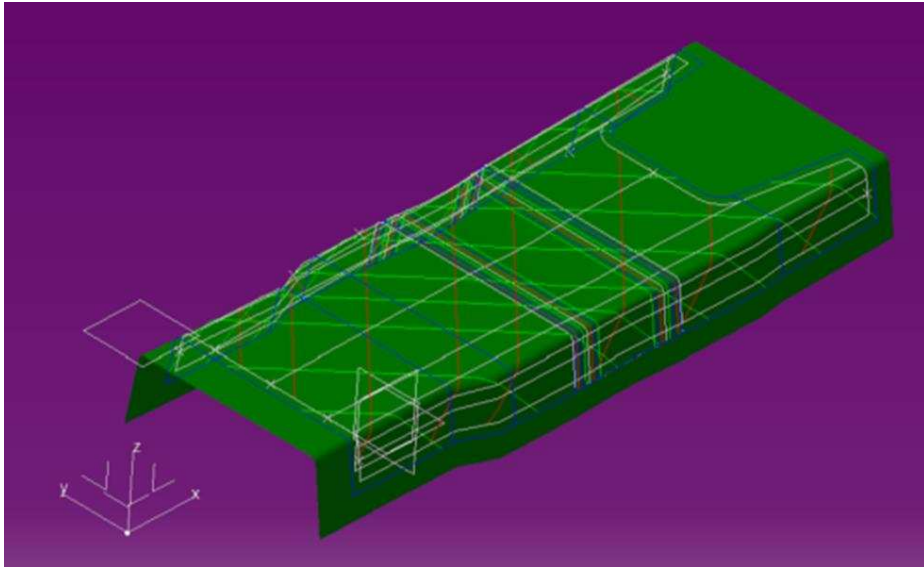


Figure 19. Spar part with multiple sections



Figure 20. Completed spar section: outer surface (left) and inner surface (right)